Holographic 3-D laser imaging into sandstone

P. Yu, M. Mustata, D. Chen, L. J. Pyrak-Nolte, and D. D. Nolte
Department of Physics, Purdue University, West Lafayette, IN, USA

Received 12 March 2002; revised 12 March 2002; accepted 9 May 2002; published 29 October 2002.

[1] With a novel imaging technique that uses holographic recording and reconstruction to perform laser-ranging into translucent media, we have imaged several grain layers into a sandstone sample. Three-dimensional microscale (10 micron lateral and 30 micron depth resolution) information on grain size and geometry was obtained as deep as 400 microns into the sample without thin-sectioning. Surficial grain features in the holographic reconstruction were associated with features observed using conventional optical and scanning electron microscopy. This imaging technique represents a new form of nondestructive evaluation of grain and pore structure in reservoir rock by acquiring full-field images at variable depths, unlike sequential scanning microscopy that requires tomographic reconstruction. *INDEX TERMS:* 5114 Physical Properties of Rocks: Permeability and porosity; 5194 Physical Properties of Rocks: Instruments and techniques; 5199 Physical Properties of Rocks: General or miscellaneous; 1894 Hydrology: Instruments and techniques; 1899 Hydrology: General or miscellaneous. **Citation:** Yu, P., M. Mustata, D. Chen, L. J. Pyrak-Nolte, and D. D. Nolte, Holographic 3-D laser imaging into sandstone, *Geophys. Res. Lett.*, *29*(20), 1988, doi:10.1029/2002GL015108, 2002.

1. Introduction

[2] The principal challenge of up-scaling techniques for multi-phase fluid dynamics in porous media is to determine which properties on the micro-scale can be used to predict macroscopic flow and spatial distribution of phases at core- and field-scales. First-principle theoretical formulations over the past decade have been derived from rigorous volume averaging theorems in which microscopic interfacial behavior is explicitly incorporated [*Muccino et al.*, 1998]. In contrast to the traditional importance placed on volume saturation, these theories have proposed that interfacial areas per volume more directly predict macroscopic behavior, and that this variable may govern the observed hysteresis in saturation-capillary pressure relationships [*Reeves and Celia*, 1996].

[3] Despite the importance of testing interfacial theories, interfacial areas per volume are considerably more difficult to measure than partial volume saturations. Volumes can be measured by simple volume displacements, by weight, or by attenuation coefficients in commercial radiation logging apparatus. Interfacial areas inside opaque rock, on the other hand, have been largely inaccessible. Most advanced imaging techniques do not have the appropriate spatial resolution to measure interfacial areas at the pore-scale. Although several imaging techniques have made inroads to this problem, such as x-ray microtomography [*Spanne et al.*, 1992; *Spanne et al.*, 1994], confocal microscopy [*Fredrich et al.*, 1995; *Montoto et al. 1995*] and metal-injection [*Pyrak-Nolte et al.*, 1997], these techniques have not previously provided information appropriate for the testing of upscaling theories.

[4] This paper describes a holographic laser-ranging technique called optical coherence imaging (OCI) that images through the first several layers of grains in a sandstone rock core. Optical coherence imaging is an advancement on optical coherence tomography (OCT) which is a well-established laser imaging technique for imaging through translucent media [*Izatt et al.*, 1997]. OCT has been most commonly applied to shallow imaging through biological tissue [*Izatt et al.*, 1996; *Pan et al.*, 1996; *Tearney et al.*, 1997]. The principal of operation for OCT relies on the coherent nature of laser light. When laser light propagates through a translucent medium, part of the light scatters off optical heterogeneities, while part continues to propagate unscattered, and reflects off buried objects of interest. This unscattered light is sometimes called "ballistic" light [*Wang et al.*, 1991].

[5] In conventional imaging scattered light obscures the image of interest carried by the ballistic light. However, the weak image-bearing light remains coherent with the original laser beam. OCT detects only the coherent image-bearing light, while rejecting the incoherent scattered light. This "coherence detection" has been demonstrated successfully in conventional OCT systems by changing the length of one of the arms in an interferometer. Light is collected from different depths in the specimen, thereby performing as a laser ranging system with the added rejection of background scattered light. Conventional OCT performs point-by-point scanning, which is not compatible with imaging directly to a video televiewer screen.

[6] We have developed a full-frame variant of OCT called optical coherence imaging. Optical coherence imaging uses the coherence of the ballistic light – and the incoherence of the unwanted obscuring light – to write an optical hologram of only the light carrying the image of interest [*Jones et al.*, 1996]. Because the coherence detector is a hologram, it captures a full image in a single shot [*Hyde et al.*, 1996]. Therefore, this penetrating-imaging system can acquire video images that can be viewed in real time on a televiewer, and recorded on a video cassette [*Jones et al.*, 1998]. This has an advantage over other penetrating-imaging processes, such as confocal microscopy, which must scan point-by-point.

[7] Previous optical coherence imaging demonstrations have been primarily used for free-space three-dimensional topography and for imaging through turbid media. No previous work has attempted to image into materials such as sandstone because of the difficulties of the strong laser

0094-8276/02/2002GL015108$05.00

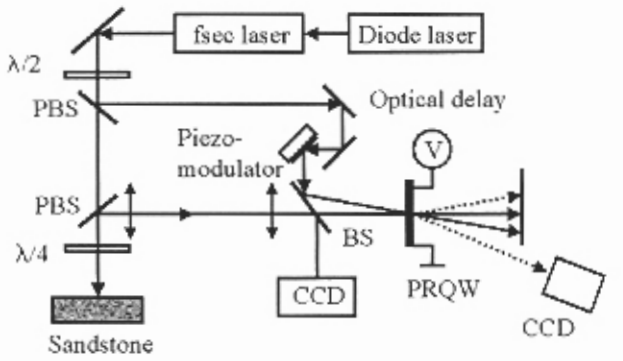

Figure 1. The experimental setup of optical coherence imaging. PBS: polarization beam splitter. BS: 50% beam splitter. PRQW: photorefractive multiple quantum well device.

speckle that arises from light scattering from static heterogeneities. In our experiments we have used a time-averaging technique to eliminate the laser speckle from the video images. The work contained in this paper represents the first application of optical coherence imaging to image into rock. We have been able to see as deep as 400 microns into the rock, and have delineated the geometric shapes of several sand grains from stacks of holographic images.

2. Experimental Methods

[8] The optical coherence imaging system (Figure 1) consists of a mode-locked Ti:sapphire laser (120 femtosecond (fs) pulses with 100 MHz repetition rate), a modified Mach Zehnder interferometer with a sample arm and a reference arm, and a photorefractive multiple quantum well device that performs as a dynamic holographic film [*Nolte*, 1999]. In the detection arm two lenses with 150 mm focal lengths form a Fourier optics system that projects a 1:1 image of the sample onto the holographic film. A spatial filter rejects part of the scattered light from the sample, and allows the ballistic components to propagate to the holographic film. The signal beam interferes with the reference beam when the optical path lengths between the signal and reference arms are matched to within a coherence length of the laser (30 microns) by adjusting the translation stage in the reference arm. The interference fringes are imprinted onto the holographic film.

[9] The holograms are reconstructed using a degenerate four-wave mixing configuration. The first-order diffracted signal from the reference beam is imaged onto the surface of a cooled CCD camera (RTE/CCD 1317, Princeton Instruments) with a 150 mm focal length lens, while an aperture is used to block the zero-order beam. The efficiency of the four-wave mixing is optimized by adjusting the wavelength and bandwidth of the laser, the size and position of the aperture, and the relative intensities between the signal and reference beams. The system has a 10 μm lateral resolution and a 30 μm depth resolution. The depth resolution is set by the coherence length of the nominal 100 fsec pulses used in the system.

[10] The choice of the intensity of the reference beam is important in order to obtain high contrast in the holograms. For the optical coherence imaging experiments on sandstone, the incident object beam (probe beam) has a power of 400 mW for a circular region with a diameter of 1.0 mm. The power of the scattered and the ballistic components from the sandstone are about 40 μW, i.e., a difference in power of four orders of magnitude. In the Fourier plane of the optical system, approximately half of the power is cut off by the spatial filter (an optical technique for rejecting scattered light). The reference beam has a power of 300 μW in a circular region with a diameter of 3.0 mm. In the optical coherence imaging experiments, an optimized ratio is achieved by synchronously adjusting the reference intensities and the spatial filter.

3. Results and Discussion

[11] The optical coherence imaging system was used to image several grain layers into a berea sandstone rock. For better understanding of the optical coherence images, we performed scanning electron microscopy (SEM) on the same region of the sample. The SEM image in (Figure 2a) was acquired using the secondary electron (SE) mode of the SEM with magnification of 50×. The contrast of the SEM image represents surface-tilt, which shows the topology of the surface of the sandstone sample. Although the SEM can acquire clear surface structure, it cannot image below the surface of the sample. Figure 2b shows an optical microgram of the same surface of the sandstone sample taken with an optical microscope at a magnification of 25×.

[12] Figure 3a shows thresholded x-y plane holograms at three different delay depths. The origin data consists of 80 holograms corresponding to increasing depth into the sample with a sampling depth step size of 10 μm. The holograms show different shapes for the different depths caused by the reflections from facets of the grains. The hologram (about 100 × 150 μm^2 in area) at the delay depth of zero in Figure 3a corresponds to the top surface of grain A that is topmost on the sandstone surface in the region. A hologram appears again in the same area at a delay depth of 222 μm representing the bottom surface of the grain. The image at the delay depth of 91 μm shows that the area corresponding to the center grain is almost dark while the white regions represent the holograms of several other grains (marked B

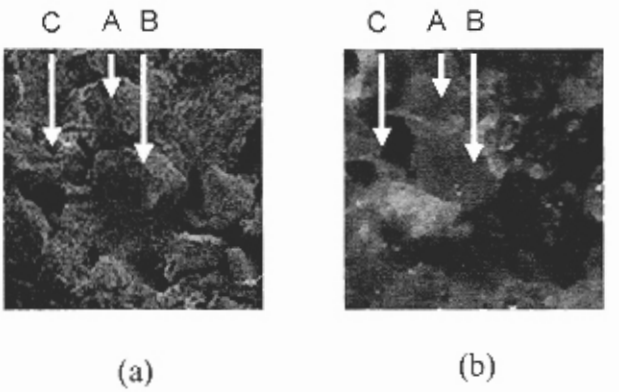

Figure 2. (a) SEM shows topology of the sandstone. The labeled grains are the selected grains for the optical coherence imaging data set, which have the same labels as in the optical microgram. (b) Optical micrograph of the sandstone.

and C). In the central dark area (labeled A), the lateral shape of the center grain is the same as the grain shape in the SEM image and optical microgram (Figure 2). Therefore, the holograms in Figure 3a show the top and bottom of the grain A, respectively. Figure 3b shows a cross section of the holograms in the x-z plane at the position of y = 300 μm. At least one tilted facet can be seen at the side of the grain in the cross section image.

[13] An important goal of this work is to obtain information on the void spaces between grains by imaging deeper than the first layer of grains. By looking for closely-spaced reflection peaks in the depth sections, it may be possible to measure the gaps between grains. Figure 4a is a cross-section of a sandstone sample in x-z plane at y = 820 μm showing considerable structure down to 500 μm deep, extending through several grains at each position. Line sections at the location x = 75 μm and 156 μm are shown in Figure 4b. Reflections indicated by arrows from the top and the bottom of grains can be seen, as well as deeper reflections from deeper grains. Though it is not possible to determine the 3D structure from a single cross-sections, the full data set contains sufficient information to fit the positions and shapes of numerous grains in the top several layers of grains in the sandstone sample.

4. Conclusion

[14] This work represents the first demonstration of optical coherence imaging (OCI) into rock. The acquired holograms provide information on the thickness of the grains (from reflections from the top and bottom surfaces of the grains) as well as information on the geometry of the grains (from reflections from the side facets of the grains). The deepest information, according to our data sets, that can be acquired is from about 400 μm beneath the surface of the sample. Calibration of the optical coherence imaging system showed that the lateral resolution of the holograms is 10 μm while the depth resolution is about 30 μm. This holographic imaging technique represents a new form microscopy that can complement or augment other conventional imaging techniques for the characterization of rock without destructive sectioning.

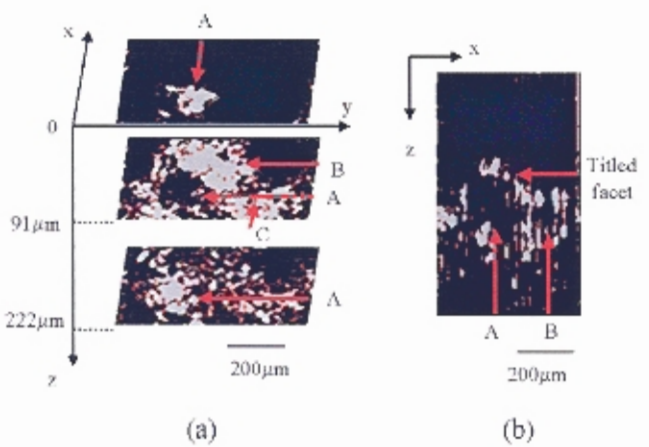

Figure 3. (a) x-y plane holograms recorded at the same region as in (Figures 2a and 2b) for different sampling depths. The bar represents the scale in the x and y axes. (b) x-z plane hologram at y = 300 μm shows the cross section of the A and B grains. The bar represents the scale in the x and z axes.

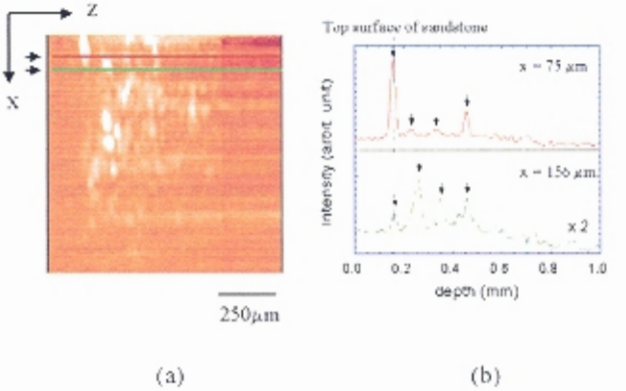

Figure 4. (a) Cross—section at location y = 820 μm with dimensions 1000 μm by 1000 μm in the x-z plane, showing considerable structure half a millimeter deep into the sandstone sample. The bar represents the scale on both x and z axes. Marked lines show where the intensity cross sections of (b) were taken. (b) Intensity cross-section through 1000 μm depth at x = 75 μm and 156 μm.

[15] **Acknowledgments.** This work is supported by DOE contract DE-AC26-99BC15207 and by NIH contract RR15040-02.

References

Fredrich, J. T., B. Menendez, and T.-F. Wong, Imaging the Pore Structure of Geomaterials, *Science*, *268*, p. 2776, 1995.

Hyde, S. C. W., R. Jones, N. P. Barry, J. C. Dainty, P. M. W. French, K. M. Kwolek, D. D. Nolte, and M. R. Melloch, Depth-resolved holography through turbid media using photorefraction, *IEEE J. Sel. Top. Quant. Electron.*, *2*, 965, 1996.

Izatt, J. A., M. D. Kulkarni, H.-W. Wang, K. Kobayashi, and M. V. Sivak, Optical coherence tomography and microscopy in gastrointestinal tissues, *IEEE J. Sel. Top. Quant. Electron.*, *2*, p. 1017, 1996.

Izatt, J. A., M. D. Kulkarni, K. Kobayashi, M. V. Sivak, J. K. Barton, and A. J. Welch, Optical Coherence Tomography, *Optics and Photonics News*, 1997.

Jones, R., S. C. W. Hyde, M. J. Lynn, N. P. Barry, J. C. Dainty, P. M. W. French, K. M. Kwolek, D. D. Nolte, and M. R. Melloch, Holographic storage and high background imaging using photorefractive multiple quantum wells, *Appl. Phys. Lett.*, *69*, 1837, 1996.

Jones, R., N. P. Barry, S. C. W. Hyde, P. M. W. French, K. M. Kwolek, D. D. Nolte, and M. R. Melloch, Direct-to-Video holographic readout in quantum wells for 3-D imaging through turbid media, *Opt. Lett.*, *23*, p. 103, 1998.

Montoto, M., A. Martinez-Nistal, A. Rodriguez-Rey, N. Fernandez-Merayo, and P. Soriano, Microfractography of granitic rocks under confocal scanning laser microscopy, *J. Microscopy*, *177*(pt. 2), 138–149, 1995.

Muccino, J. C., W. G. Gray, and L. A. Ferrand, Toward and improved understanding of multiphase flow in porous media, *Rev. Geophys.*, in press, 1998.

Nolte, D. D., Optoelectronic Properties of Semi-insulating Heterostructures, *J. Appl. Phys.*, *85*, 6259, 1999.

Pan, Y., E. Lankenau, J. Welzel, R. Birngruber, and R. Engelhardt, Optical coherence gated imaging of biological tissues, *IEEE J. Sel. Top. Quantum Electron.*, *2*, p. 1029, 1996.

Pyrak-Nolte, L. J., C. D. Montemagno, and D. D. Nolte, Volumetric imaging of aperture distributions in connected fracture networks, *Geophysical Research Letters*, *24*(18), p. 2343–2346, 1997.

Reeves, P. C., and M. A. Celia, A functional relationship between capillary pressure, saturation, and interfacial area as revealed by a pore-scale network model, *Water Resources Research*, *32*(8), 2345–2358, 1996.

Spanne, P., K. W. Jones, M. L. Rivers, E. R. Sutton, S. R. Brown, W. B. Lindquist, and S. M. Lee, Synchrotron computed microtomography analysis of drill core specimens, *I. Experimental, EOS, 73*(14), 308, 1992.

Spanne, P., J. F. Thovert, C. J. Jacquin, W. B. Lindquist, K. W. Jones, and P. M. Adler, Synchrotron computed microtomography of porous media: Topology and transport, *Physical Review Letters, 73*(14), 2001--2004, 1994.

Tearney, G. J., M. E. Brazinski, B. E. Bouma, S. A. Boppart, C. Pitris, J. F. Southern, and J. G. Fujimoto, In Vivo endoscopic optical biopsy with optical coherence tomography, *Science, 276*, 2037, 1997.

Wang, L., P. P. Ho, C. Liu, G. Zhang, and R. R. Alfano, Ballistic 2-D imaging through scattering walls using an ultrafast Optical Kerr gate, *Science, 253*, 769, 1991.

P. Yu, M. Mustata, D. Chen, L. J. Pyrak-Nolte, and D. D. Nolte, Department of Physics, Purdue University, West Lafayette, IN 47907, USA.